

## ERROR ESTIMATION AND ADAPTIVITY FOR NONLINEAR FE ANALYSIS

ANTONIO HUERTA\*, ANTONIO RODRÍGUEZ-FERRAN\*  
PEDRO DÍEZ\*

\* Departament de Matemàtica Aplicada III, E.T.S. de Ingenieros de Caminos,  
Edifici C2, Campus Nord, Universitat Politècnica de Catalunya,  
E-08034 Barcelona, Spain,  
e-mail: antonio.huerta@upc.es

An adaptive strategy for nonlinear finite-element analysis, based on the combination of error estimation and  $h$ -remeshing, is presented. Its two main ingredients are a residual-type error estimator and an unstructured quadrilateral mesh generator. The error estimator is based on simple local computations over the elements and the so-called patches. In contrast to other residual estimators, no flux splitting is required. The adaptive strategy is illustrated by means of a complex nonlinear problem: the failure analysis of a single-edge notched beam. The quasi-brittle response of concrete is modelled by means of a nonlocal damage model.

**Keywords:** finite elements, error estimation, adaptivity, nonlinearity, quality of FE solutions, damage models

### 1. Introduction

Adaptive strategies are nowadays a standard tool in practical finite-element computations. For any problem, adaptivity is an essential tool to obtain numerical solutions with a controlled accuracy. For some problems (typically in nonlinear domains), adaptive strategies are even more fundamental: without them, a finite-element solution simply cannot be computed. This is the case, e.g., with problems in nonlinear solid mechanics involving large strains or localization.

Two main ingredients of an adaptive procedure are (a) a tool for assessing the error of the solution computed with a given mesh and (b) an algorithm to define a new spatial discretization (Huerta *et al.*, 1999).

Two different approaches can be used for assessing the error: error estimators or error indicators. Error estimators approximate a measure of the actual error in a given norm. Error indicators, on the other hand, are based on heuristic considerations. For each particular application, a readily available quantity is chosen, in an *ad hoc* manner, as an error indicator.

The second ingredient of an adaptive procedure is the definition of a new spatial discretization. The goal is to increase or decrease the richness of the interpolation according to the output of the error assessment. Three main types of strategies can be used:  $h$ -adaptivity,  $p$ -adaptivity and  $r$ -adaptivity. The  $h$ -adaptivity consists in changing the size of the finite elements. In  $p$ -adaptivity, the degree of the interpolating polynomials is increased. The

$r$ -adaptivity consists in relocating the nodes, without changing the mesh connectivity.

This paper discusses the combination of error estimators and  $h$ -adaptivity. A general overview of adaptive strategies can be found in (Huerta *et al.*, 1999).

Error estimators for linear problems are standard and perform well (Strouboulis and Haque, 1992a; 1992b). Error estimators can be classified mainly into two groups: (a) flux projection or ZZ-like error estimators (Zienkiewicz and Zhu, 1987) and (b) residual type error estimators (Ainsworth and Oden, 1993; Bank and Weiser, 1985; Ladevèze *et al.*, 1991), see also (Zhu, 1997) for a study of their relationship. Many nonlinear generalizations have been defined from linear estimators. Nevertheless, most of them lose the sound theoretical basis of the linear counterpart because they are based on properties that stand only for linear problems (Chow and Carey, 1993; Fourment and Chenot, 1995; Gallimard *et al.*, 1996; Ladevèze and Rougeot, 1997; Ortiz and Quigley, 1991; Zienkiewicz and Huang, 1990).

Here, a residual estimator for linear and nonlinear problems is discussed (Díez *et al.*, 1998; Huerta and Díez, 2000). The performance of this estimator does not depend on superconvergence properties, which have only been proved for linear problems. Moreover, the presented approach can be applied to general unstructured meshes with different element types (for instance, triangles and quadrilaterals). Consequently, assuming that a sound equation for the error is provided, this estimator is easily applied to

nonlinear problems. Here the nonlinear error equation is linearized by means of a tangent Taylor expansion.

The remainder of the paper is structured as follows. Section 2 states the problem and introduces the notation. In Section 3 the philosophy and the mechanism of the linear error estimator introduced in (Díez *et al.*, 1998) are described. The presentation of the linear estimator is oriented to extending it easily to the nonlinear case (Huerta and Díez, 2000), as is discussed in Section 4. The nonlinear error estimator is then combined with  $h$ -remeshing to provide an adaptive strategy, see Section 5, which is illustrated by means of some numerical examples in Section 6. The examples deal with the failure of concrete structures. Finally, Section 7 contains some concluding remarks.

## 2. Model Problem

Let  $\Omega$  be a bounded domain in  $\mathbb{R}^2$  with a smooth boundary  $\partial\Omega$ . The boundary  $\partial\Omega$  is divided into two parts  $\Gamma_D$  and  $\Gamma_N$  such that  $\partial\Omega = \bar{\Gamma}_D \cup \bar{\Gamma}_N$  and  $\Gamma_D \cap \Gamma_N = \emptyset$ . The standard Sobolev space

$$H_{\Gamma_D}^1(\Omega) := \{v \in H^1(\Omega) \text{ such that } v = 0 \text{ on } \Gamma_D\}$$

is introduced as the natural space containing the underlying functions. The unknown function  $u$  is the solution to the following boundary-value problem: Find  $u$  in  $H_{\Gamma_D}^1(\Omega)$  such that

$$a(u, v) = l(v) \quad \text{for all } v \in H_{\Gamma_D}^1(\Omega), \quad (1)$$

where the forms  $a(\cdot, \cdot)$  and  $l(\cdot)$  are defined in  $H_{\Gamma_D}^1(\Omega) \times H_{\Gamma_D}^1(\Omega)$  and  $H_{\Gamma_D}^1(\Omega)$ , respectively.

**Remark 1.** Although  $u$  belongs to  $H_{\Gamma_D}^1(\Omega)$  (i.e.  $u = 0$  on  $\Gamma_D$ ), the Dirichlet boundary conditions on  $\Gamma_D$  in the original boundary value problem may be non-homogeneous.

The form  $a(\cdot, \cdot)$  is linear with respect to its second argument. In linear problems,  $a(\cdot, \cdot)$  is bilinear. In particular, for second-order linear self-adjoint problems,  $a(\cdot, \cdot)$  is bilinear and symmetric. Moreover, in many problems (e.g. in linear elasticity),  $a(\cdot, \cdot)$  is also positive definite and, hence, it is a scalar product.

The Galerkin finite-element method provides an approximation  $u_h$  to  $u$ , lying in a finite-dimensional space  $V_h \subset H_{\Gamma_D}^1(\Omega)$  and satisfying

$$a(u_h, v_h) = l(v_h) \quad \text{for all } v_h \in V_h. \quad (2)$$

The finite-dimensional space  $V_h$  is associated with a finite-element mesh of characteristic size  $h$ . The elements of this mesh are denoted by  $\Omega_k$ ,  $k = 1, 2, \dots$  and it is assumed that  $\bar{\Omega} = \bigcup_k \bar{\Omega}_k$ .

The goal of *a-posteriori* error estimation is to assess the accuracy of the approximate solution  $u_h$ . This is done by analyzing the error  $e := u - u_h$  and estimating both global and local measures of the error. The local measures are used to describe the spatial distribution of the error, and the global measure, which is employed to verify the acceptability criterion, is obtained by summing up the local contributions.

Thus a norm to measure the error must be defined. One of the most popular options (in the linear case) is the energy norm induced by  $a(\cdot, \cdot)$ :

$$\|e\| := [a(e, e)]^{1/2}. \quad (3)$$

The reasons for choosing  $\|\cdot\|$  are as follows: it has physical meaning, it is equivalent to standard Sobolev norms and it can be easily restricted in order to obtain associated local norms.

In the following, the restriction of  $a(\cdot, \cdot)$  to the element  $\Omega_k$  ( $k = 1, 2, \dots$ ) of the mesh is denoted by  $a_k(\cdot, \cdot)$ . Thus the restriction of  $\|\cdot\|$  to  $\Omega_k$ ,  $\|\cdot\|_k$ , is induced by  $a_k(\cdot, \cdot)$ . The value of  $\|e\|_k$  in each element must be estimated in order to describe the spatial distribution of  $e$ . A suitable extension of the linear estimator maintaining most of its properties is defined for the nonlinear case.

## 3. Linear A-Posteriori Error Estimation

Typically, for linear elasticity, linear heat diffusion, etc.,  $a(\cdot, \cdot)$  is a scalar product. Then  $u_h$  is the projection of  $u$  on  $V_h$  and the error  $e = u - u_h$  is orthogonal to  $V_h$  in the sense of  $a(\cdot, \cdot)$ . As has previously been said, the objective of this error estimator is to assess both a global value of the error and its spatial distribution.

Assuming that  $a(\cdot, \cdot)$  is bilinear, (1) can be easily rearranged to obtain a weak equation for the error. The error  $e$  is the element in  $H_{\Gamma_D}^1(\Omega)$  that satisfies

$$a(e, v) = l(v) - a(u_h, v) \quad \text{for all } v \in H_{\Gamma_D}^1(\Omega). \quad (4)$$

Note that the right-hand side of (4) is a residual term which accounts for the nonsatisfaction of (1).

### 3.1. The Reference Error

The error  $e$  is unknown and it is impossible to obtain its exact value. Thus the only attainable goal is to obtain an approximation to  $e$ , say  $e_{\tilde{h}}$ . This approximation to the error can be easily defined from a new approximation to  $u$ , say  $u_{\tilde{h}}$ , more accurate than  $u_h$ . For instance,  $u_{\tilde{h}}$  may be a finite element approximation associated with a finer mesh of characteristic size  $\tilde{h}$  ( $\tilde{h} \ll h$ ). The associated interpolation space  $V_{\tilde{h}}$  is much richer than  $V_h$ . Then  $u_{\tilde{h}}$

is much more precise than  $u_h$  and, therefore,  $e_{\tilde{h}} := u_{\tilde{h}} - u_h$  is a good approximation of  $e$ . This is formally shown in (Oden *et al.*, 1989) as a consequence of the *a-priori* convergence analysis of the finite-element method.

**Remark 2.** The *a-priori* error analysis of the finite-element method gives error bounds like (Hughes, 1987)

$$\|e\| = \|u - u_h\| \leq Ch^p \quad \text{and} \quad \|u - u_{\tilde{h}}\| \leq C\tilde{h}^p, \quad (5)$$

where  $p$  stands for the degree of the interpolating polynomial. Applying Richardson extrapolation and the orthogonality between  $e_{\tilde{h}}$  and  $u - u_{\tilde{h}}$ , we can show that

$$\|u_{\tilde{h}} - u_h\| = \|e_{\tilde{h}}\| \simeq \left[ 1 - \left( \frac{\tilde{h}}{h} \right)^{2p} \right]^{1/2} \|e\|. \quad (6)$$

That is, if  $\tilde{h}$  is one fourth of  $h$  and  $p$  is one, the reference error,  $e_{\tilde{h}}$ , is 97% of the actual error  $e$ .

In the following, the finer mesh of element size  $\tilde{h}$  is denoted as the reference mesh, as well as the associated solution,  $u_{\tilde{h}}$  is the reference solution and  $e_{\tilde{h}}$  is the reference error. Note that the discretization can be enriched using different strategies: instead of the  $h$ -refinement approach (reduce the element size), the  $p$ -refinement approach (increase the degree of the interpolation polynomial) can also be used to increase the accuracy of the interpolation and define a reference solution. Here, for the simplicity of presentation, only the  $h$ -refinement approach is presented.

In fact, computing  $u_{\tilde{h}}$  and then obtaining  $e_{\tilde{h}}$  is equivalent to directly solving the error equation (4) using the finer mesh. That is, solving (1) using  $V_{\tilde{h}}$  is equivalent to solving (4) using the same interpolation space. Thus  $e_{\tilde{h}}$  is the element of  $V_{\tilde{h}}$  that satisfies

$$a(e_{\tilde{h}}, v_{\tilde{h}}) = l(v_{\tilde{h}}) - a(u_h, v_{\tilde{h}}) \quad \text{for all } v_{\tilde{h}} \in V_{\tilde{h}}. \quad (7)$$

Nevertheless, the standard computation of  $e_{\tilde{h}}$  must be avoided due to its prohibitive computational cost: the refined mesh generating  $V_{\tilde{h}}$  has a number of degrees of freedom much larger than the original mesh and, therefore, the cost of computing  $e_{\tilde{h}}$  is usually prohibitive.

In the remainder of this section a method for approximating  $e_{\tilde{h}}$  by low-cost local computations is presented. This method is split into two phases. First, a simple residual problem is solved inside each element and an interior estimate is obtained. Second, a new family of simple problems is considered and the interior estimate is complemented adding a new contribution. The first phase is called interior estimation and the second is called patch estimation.

### 3.2. Interior Estimation

Solving the global reference problem, see eqn. (7), implies the solution of a very large system of equations with a prohibitive computational cost. In order to avoid unaffordable computations, the error estimation must be performed solving local problems. In fact, standard residual-type error estimators solve elementary problems because the natural partition of the domain is the set of elements of the “coarse” computational mesh,  $\Omega_k$ ,  $k = 1, 2, \dots$

Here, each element  $\Omega_k$  is discretized by an elementary submesh built from a discretization of the reference element and mapped into  $\Omega_k$ , see Fig. 1. Then the reference mesh is constructed by the assembly of the elementary submeshes discretizing each element, see Fig. 2. That is, each element  $\Omega_k$  of the mesh is associated with a local interpolation space  $V_{\tilde{h},k}$ , induced by the corresponding elementary submesh. In fact, this space  $V_{\tilde{h},k}$  is a finite-dimensional subset of  $H^1(\Omega_k)$ . Notice that the functional space  $\bigoplus_k V_{\tilde{h},k}$  does not coincide with  $V_{\tilde{h}}$  because the former includes functions which are discontinuous along the element edges.

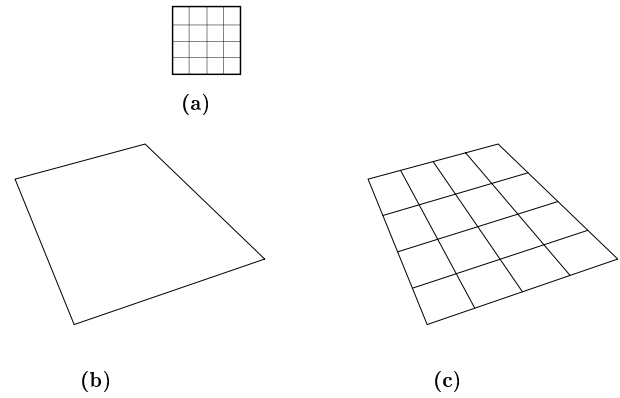


Fig. 1. (a) The reference submesh is mapped into (b) an element to get (c) an elementary submesh.

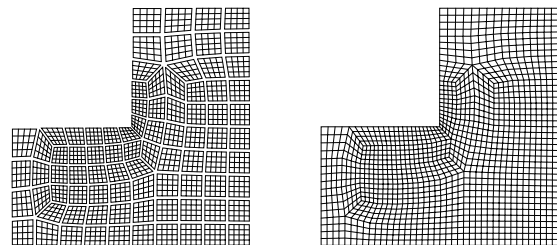


Fig. 2. A set of elementary submeshes and the associated reference mesh.

Then the elementary submeshes can be used to solve the error equation, see (4), on each element  $\Omega_k$  of the original mesh. However, the solution of such problems requires proper boundary conditions for the error. Most residual type error estimators (Ainsworth and Oden, 1993; Bank and Weiser, 1985; Ladevèze *et al.*, 1991), solve (4) by prescribing the flux around each element  $\Omega_k$ , that is, by solving pure Neumann problems. The prescribed values of error fluxes are found by splitting the jump of the fluxes of  $u_h$  across the element edges. The computation of the flux jumps across the edges is expensive. The splitting procedure usually equilibrates the fluxes around the element and therefore is generally involved.

In this work, the elementary problems are solved in a straightforward manner by imposing homogeneous Dirichlet conditions for the error, along the boundary of each element  $\Omega_k$  (Díez *et al.*, 1998). That is, the approximation to the error is prescribed to zero at all the boundary nodes of the elementary submesh. In other words, the local problem is solved in the interpolation space  $V_{\bar{h},k,0} := V_{\bar{h},k} \cap H_0^1(\Omega_k)$ , where  $H_0^1(\Omega_k) := \{v \in H^1(\Omega_k) \text{ such that } v = 0 \text{ in } \partial\Omega_k \setminus (\partial\Omega_k \cap \Gamma_N)\}$ . The functions in  $V_{\bar{h},k,0}$  have their support in  $\Omega_k$  but they can be continuously extended in the whole domain  $\Omega$  by setting them to zero elsewhere (i.e. in  $\Omega \setminus \Omega_k$ ). In the remainder of the paper the same notation is used for every local function and its continuous extension. In that sense,  $V_{\bar{h},k,0}$  is also seen as a subspace of  $H_{\Gamma_D}^1(\Omega)$ . Thus,  $a(\cdot, \cdot)$  may apply to elements in  $V_{\bar{h},k,0}$  and, in this case, it coincides with  $a_k(\cdot, \cdot)$ . This allows us to write the local elementary problem using only the global forms  $a(\cdot, \cdot)$  and  $l(\cdot)$ . The solution to this local problem is the function  $\varepsilon_k$  satisfying

$$a(\varepsilon_k, v_{\bar{h}}) = l(v_{\bar{h}}) - a(u_h, v_{\bar{h}}) \quad \text{for all } v_{\bar{h}} \in V_{\bar{h},k,0}. \quad (8)$$

**Remark 3.** According to the definition of  $V_{\bar{h},k,0}$ , the error is set to zero on  $\Gamma_D$  (which is a true condition because  $u_h$  is equal to  $u$  on  $\Gamma_D$ , up to the accuracy of the discretization), but also on the interior element boundaries (where it is unknown). That is, the error is artificially set to zero along the (interior) inter-element boundaries. Notice that the flux of the error can be computed on  $\Gamma_N$  and this condition is implicitly imposed in (8) via the residual right-hand-side term.

**Remark 4.** Assuming that  $a(\cdot, \cdot)$  is a scalar product,  $\varepsilon_k$  is the projection of  $e_{\bar{h}}$  (and  $e$ ) onto  $V_{\bar{h},k,0}$ . Thus  $e_{\bar{h}} - \varepsilon_k$  (and  $e - \varepsilon_k$ ) is orthogonal to every element in  $V_{\bar{h},k,0}$  and, in particular,  $a(e_{\bar{h}} - \varepsilon_k, \varepsilon_k) = a(e - \varepsilon_k, \varepsilon_k) = 0$ . This orthogonality condition is satisfied even locally, i.e.  $a_k(e_{\bar{h}} - \varepsilon_k, \varepsilon_k) = a_k(e - \varepsilon_k, \varepsilon_k) = 0$  because, as has previously been said,  $a(\cdot, \cdot)$  coincides with  $a_k(\cdot, \cdot)$  if at least one of the arguments has compact support in  $\Omega_k$ .

This discrete local problem leads to the following system of equations:

$$\mathbf{K}_{\bar{h},k}^e \varepsilon_k = \mathbf{r}_k^e, \quad (9)$$

where  $\mathbf{K}_{\bar{h},k}^e$  is the stiffness matrix resulting from discretizing  $a(\cdot, \cdot)$  in a basis of  $V_{\bar{h},k,0}$  which is the set of the standard finite-element interpolation functions associated with the elementary submesh. The column vector  $\mathbf{r}_k^e$  results from discretizing the residual form  $l(\cdot) - a(u_h, \cdot)$ , cf. (8), in the same basis. The vector  $\varepsilon_k$  is the expression of  $\varepsilon_k$  in the chosen basis. The local energy norm of the interior estimate  $\varepsilon_k$  can be directly computed since

$$\|\varepsilon_k\|^2 = a(\varepsilon_k, \varepsilon_k) = \varepsilon_k^T \mathbf{K}_{\bar{h},k}^e \varepsilon_k = \varepsilon_k^T \mathbf{r}_k^e. \quad (10)$$

Thus, since  $\varepsilon_k$  has its support in  $\Omega_k$ , local and global norms are equal:  $\|\varepsilon_k\| = \|\varepsilon_k\|_k$ . Recall that the local restriction of the norm  $\|\cdot\|$  to the element  $\Omega_k$ ,  $\|\cdot\|_k$ , is used to obtain elementary measures of the error and to describe the error distribution.

Once the elementary problems are solved, the local interior estimates can be assembled to build up a global estimate  $\varepsilon$  having values in the whole domain  $\Omega$ ,

$$\varepsilon = \sum_k \varepsilon_k. \quad (11)$$

The interior estimates  $\varepsilon_k$  and  $\varepsilon_{k'}$  associated with different elements ( $k \neq k'$ ) are orthogonal because they have disjoint supports ( $\Omega_k \cap \Omega_{k'} = \emptyset$ ). Then the Pythagoras theorem holds and the norm of  $\varepsilon$  can be easily computed:

$$\|\varepsilon\|^2 = \sum_k \|\varepsilon_k\|^2. \quad (12)$$

Both local,  $\varepsilon_k$ , and global,  $\varepsilon$ , interior estimates are projections of  $e$  (and also of  $e_{\bar{h}}$ ) onto the respective subspaces  $V_{\bar{h},k,0}$  and  $\bigoplus_k V_{\bar{h},k,0}$ , which are included in  $V_{\bar{h}}$  (the inclusion in  $V_{\bar{h}}$  is satisfied because of the homogeneous Dirichlet boundary condition, which preserves the global continuity: note that  $V_{\bar{h},k,0} \subset V_{\bar{h}}$  and  $\bigoplus_k V_{\bar{h},k,0} \subset V_{\bar{h}}$ ). Consequently, the norm of the interior estimate is a lower bound of the actual and reference errors:

$$\|\varepsilon\| \leq \|e_{\bar{h}}\| \leq \|e\|. \quad (13)$$

Moreover, the local estimates are also lower bounds of the actual and the reference local errors, i.e. we have the following result:

**Proposition 1.**

$$\|\varepsilon_k\|_k \leq \|e_{\bar{h}}\|_k, \quad \|\varepsilon_k\|_k \leq \|e\|_k.$$

*Proof.* These inequalities are proven using the local orthogonality conditions formulated in Remark 4, see (Díez *et al.*, 1998):

$$\begin{aligned}
 \|e_{\bar{h}}\|_k^2 &= a_k(e_{\bar{h}}, e_{\bar{h}}) \\
 &= a_k([e_{\bar{h}} - \varepsilon_k] + \varepsilon_k, [e_{\bar{h}} - \varepsilon_k] + \varepsilon_k) \\
 &= \|e_{\bar{h}} - \varepsilon_k\|_k^2 + \|\varepsilon_k\|_k^2 + \underbrace{2a_k(e_{\bar{h}} - \varepsilon_k, \varepsilon_k)}_{=0} \\
 &\geq \|\varepsilon_k\|_k^2.
 \end{aligned}$$

The same rationale is used to prove that  $\|\varepsilon_k\|_k \leq \|e\|_k$ . ■

The choice of the artificial boundary condition may imply that  $\|\varepsilon\| \ll \|e\|$ . This is a consequence of forcing the approximation  $\varepsilon$  to be zero along the inter-element boundaries. Since the reference error  $e_{\bar{h}}$  is generally nonzero at all these points,  $\varepsilon$  may be a poor approximation to  $e_{\bar{h}}$ . In other words, interior residuals are considered in the right-hand-side term of (8) but the information contained in the flux jumps is ignored.

### 3.3. Patch Estimation and Complete Estimate

Once the interior estimate is computed, a new contribution must be added in order to account for the flux jumps. This is equivalent to improving the error estimation by adding nonzero values in the inter-element boundaries. In this section, this is done by following the same idea of the interior estimation, precluding the direct computation of flux jumps and avoiding the flux splitting procedure.

The interior estimate is based on solving local problems within the elements  $\Omega_k$ ,  $k = 1, 2, \dots$ . But other partitions can also be used: let us consider a new family of disjoint subdomains  $(\Lambda_l, l = 1, 2, \dots)$  covering  $\Omega$ . Each of these subdomains  $\Lambda_l$  overlaps a number of elements. Moreover, these subdomains include the inter-element boundaries. In order to simplify the exposition, in the following the subdomains  $\Lambda_l$  are called patches. Using the elementary submeshes of Fig. 1, the most natural choice for patch subdomains is to associate them with the nodes of the mesh: each patch is associated with a node and includes a fourth of every element sharing that node (see Fig. 3 for an illustration and (Díez *et al.*, 1998) for a detailed presentation).

Each patch submesh induces an interpolation subspace  $U_{\bar{h},l}$ . The space  $U_{\bar{h},l}$  is associated with  $\Lambda_l$  in the same way as  $V_{\bar{h},k}$  is associated with  $\Omega_k$ . In order to impose local boundary conditions,  $e_{\bar{h}}$  is approximated in  $U_{\bar{h},l,0} := U_{\bar{h},l} \cap H_0^1(\Lambda_l)$ , where  $H_0^1(\Lambda_l) := \{v \in H^1(\Lambda_l) \text{ such that } v = 0 \text{ in } \partial\Lambda_l \setminus (\partial\Lambda_l \cap \Gamma_N)\}$ . Thus, over each patch  $\Lambda_l$ , a new local estimate  $\eta_l$  is computed

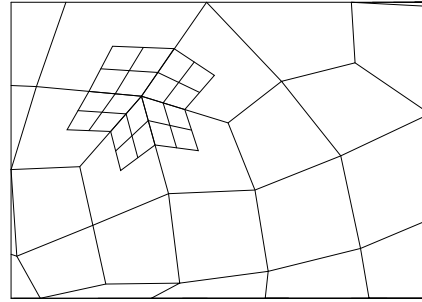


Fig. 3. A patch submesh centred in a node of the computational mesh.

such that it belongs to  $U_{\bar{h},l,0}$  and satisfies

$$a(\eta_l, v_{\bar{h}}) = l(v_{\bar{h}}) - a(u_h, v_{\bar{h}}) \quad \text{for all } v_{\bar{h}} \in U_{\bar{h},l,0}. \quad (14)$$

Equation (14) can also be written in a matrix form analogous to (9), i.e.

$$\mathbf{K}_{\bar{h},l}^p \boldsymbol{\eta}_l = \mathbf{r}_l^p, \quad (15)$$

where the matrix  $\mathbf{K}_{\bar{h},l}^p$  and the vectors  $\boldsymbol{\eta}_l$  and  $\mathbf{r}_l^p$  are the expressions of  $a(\cdot, \cdot)$ ,  $\eta_l$  and  $l(\cdot) - a(u_h, \cdot)$  in a basis of  $U_{\bar{h},l,0}$ , respectively. Thus the norm of  $\eta_l$  can be easily computed as

$$\|\eta_l\|^2 = \boldsymbol{\eta}_l^T \mathbf{r}_l^p \quad (16)$$

and, again, the local estimates can be assembled to build up a global estimate having values in the whole domain  $\Omega$ :

$$\eta = \sum_l \eta_l. \quad (17)$$

The norm of  $\eta$  can be easily computed, due to the orthogonality of the different spaces  $U_{\bar{h},l,0}$  (the patches are disjoint):

$$\|\eta\|^2 = \sum_l \|\eta_l\|^2. \quad (18)$$

Nevertheless, the norm of  $\eta$  cannot be directly added to the norm of the interior estimate  $\varepsilon$  because  $\eta$  and  $\varepsilon$  are not orthogonal. In order to easily add the two contributions,  $\eta$  is forced to be orthogonal to  $\varepsilon$ . That is, an additional condition to each  $\eta_l$  is imposed in (14). This orthogonality condition is written as

$$a(\varepsilon, \eta_l) = 0, \quad (19)$$

and can also be seen as a linear restriction to the vector  $\boldsymbol{\eta}_l$  in (15):

$$\boldsymbol{\varepsilon}^T \mathbf{K}_{\bar{h},l}^p \boldsymbol{\eta}_l = 0. \quad (20)$$

**Remark 5.** The orthogonality condition of (20) is a linear restriction and can be imposed either *a priori*, modifying the system of equations (15), or *a posteriori*, solving the

original equation (15) and modifying the result. The former option seems to be more natural, since it corresponds to projection onto a restricted space and is easily implemented using the Lagrange multiplier technique. The latter option consists in freely projecting  $e_{\tilde{h}}$  onto  $U_{\tilde{h},l,0}$ , i.e. solving (15), and then subtracting the projection of the result on  $\text{span}\langle\varepsilon\rangle$ . Thus a free projection, say  $\eta_l^{\text{free}}$ , is computed first and, then, the restricted one,  $\eta_l$ , is obtained as

$$\eta_l = \eta_l^{\text{free}} - \frac{a(\eta_l^{\text{free}}, \varepsilon)}{a(\varepsilon, \varepsilon)} \varepsilon.$$

Thus  $\eta$  is computed using the orthogonality condition of (19) or (20) and the patch estimate  $\eta$  can be added to the interior estimate  $\varepsilon$  to build up an approximation to the reference error having values in the whole domain  $\Omega$ :

$$e_{\tilde{h}} \simeq e_L := \varepsilon + \eta. \quad (21)$$

This estimate is denoted by  $e_L$  because it is obtained by performing only local computations. The global and local norms of  $e_L$  can be easily computed:

$$\|e_L\|^2 = \|\varepsilon\|^2 + \|\eta\|^2 \quad (22)$$

and

$$\|e_L\|_k^2 = \|\varepsilon\|_k^2 + \|\eta\|_k^2 = \|\varepsilon\|_k^2 + \sum_l \|\eta_l\|_k^2. \quad (23)$$

Notice that in the sum of (23) the subscript  $l$  ranges only the values such that  $\Lambda_l$  overlaps  $\Omega_k$ , i.e.  $\Lambda_l \cap \Omega_k \neq \emptyset$ , see (Díez et al., 1998).

The global measure of the local estimate maintains the lower bound properties, i.e.  $\|e_L\| \leq \|e_{\tilde{h}}\|$  because  $e_L$  is the projection of  $e_{\tilde{h}}$  (and  $e$ ) onto a subspace of  $V_{\tilde{h}}$ , see (Díez et al., 1998) for a geometrical interpretation. This subspace is  $\text{span}\langle\varepsilon\rangle \oplus \left\{ \left[ \bigoplus_l U_{\tilde{h},l,0} \right] \cap \text{span}\langle\varepsilon\rangle^\perp \right\}$ . In fact,  $\varepsilon$  is the projection of  $e_{\tilde{h}}$  (and  $e$ ) onto  $\text{span}\langle\varepsilon\rangle$  and  $\eta$  is the projection of  $e_{\tilde{h}}$  (and  $e$ ) onto  $\left\{ \left[ \bigoplus_l U_{\tilde{h},l,0} \right] \cap \text{span}\langle\varepsilon\rangle^\perp \right\}$ . These subspaces are obviously orthogonal and, consequently,  $e_L = \varepsilon + \eta$  is the projection of  $e_{\tilde{h}}$  (and  $e$ ) on  $\text{span}\langle\varepsilon\rangle \oplus \left\{ \left[ \bigoplus_l U_{\tilde{h},l,0} \right] \cap \text{span}\langle\varepsilon\rangle^\perp \right\}$ . Moreover, taking into account the contribution of the patches, the complete estimate  $\|e_L\|$  is a quite good approximation of the reference error  $\|e_{\tilde{h}}\|$  (and also of the actual error  $\|e\|$ ). An analysis of the efficiency of this estimator can be found in (Díez and Egozcue, 2001).

## 4. Nonlinear Generalization

### Fully Nonlinear Problem

If the problem is nonlinear, the first argument of the form  $a(\cdot, \cdot)$  is nonlinear, i.e.

$$a(e + u_h, v) \neq a(e, v) + a(u_h, v). \quad (24)$$

This case includes general sources of nonlinearity. For instance, in mechanical problems, both material (associated with the constitutive model) and geometric nonlinearities are accounted for.

Consequently, the linear error equation (4) is not valid anymore. In fact, the only available equation for the error is found by rewriting (1):

$$a(e + u_h, v) = l(v) \quad \text{for all } v \in V. \quad (25)$$

This equation is associated with a reference error  $e_{\tilde{h}}$  in  $V_{\tilde{h}}$  which could be computed using the reference mesh:

$$a(e_{\tilde{h}} + u_h, v_{\tilde{h}}) = l(v_{\tilde{h}}) \quad \text{for all } v_{\tilde{h}} \in V_{\tilde{h}}. \quad (26)$$

This is unaffordable from a computational point of view, especially for nonlinear problems. A method for approximating  $e_{\tilde{h}}$  by local inexpensive computations is introduced in (Díez et al., 2000) for mechanical problems. This method follows the main philosophy of the linear estimator presented in the previous section. Thus, firstly,  $e_{\tilde{h}}$  is approximated by solving elementary problems subject to homogeneous Dirichlet-type boundary conditions (interior estimate), and secondly, the estimate is completed by adding the contribution of a new set of approximations defined over a family of subdomains denoted as patches.

Nevertheless, (26) can often be simplified and an approximate linear equation for the error is obtained. This is very useful because once a linear error equation is found, the philosophy and the structure of the linear estimator presented in the previous section can be extended to nonlinear problems in a straightforward manner. This extension is presented in the remainder of this section.

### Tangent Approximation and Nonlinear Error Estimation

The error is assumed to be small compared with the solution. This is also valid for the reference error, i.e.  $\|e_{\tilde{h}}\| \ll \|u_h\|$ . Thus the first argument of  $a(\cdot, \cdot)$ , which is a nonlinear function, can be properly approximated using a tangent expansion around  $u_h$ , see (Ciarlet, 1983):

$$a(e + u_h, v) \approx a(u_h, v) + a_T(u_h; e, v), \quad (27)$$

where  $a_T(u_h; \cdot, \cdot)$  is the linear approximation to  $a(\cdot, \cdot)$  around  $u_h$ .

By substituting (27) into (25), an approximation for the error equation is found:

$$a_T(u_h; e, v) = l(v) - a(u_h, v) \quad \text{for all } v \in H_{\Gamma_D}^1(\Omega). \quad (28)$$

Equation (28) is linear and very similar to (4): the right-hand-side residual terms are identical. However, the left-hand-side terms are different because of the tangent form of (28).

The reference error equation can be obtained by discretizing (28). This allows us to characterize the reference error  $e_{\tilde{h}}$  as the solution of the linear problem:

$$a_T(u_h; e_{\tilde{h}}, v_{\tilde{h}}) = l(v_{\tilde{h}}) - a(u_h, v_{\tilde{h}}) \quad \text{for all } v_{\tilde{h}} \in V_{\tilde{h}}, \quad (29)$$

which is analogous to (7). Although the original problem and, hence, the error equation (27) are nonlinear, (29) is a linear system of equations. In fact, the matrix of this linear system of equations, which is associated with the bilinear form  $a_T(u_h; \cdot, \cdot)$ , is the standard tangent matrix. Notice that the tangent matrix (or its approximation) is typically available in finite-element codes. The linear system of equations (29) is still unaffordable because of its size. Nevertheless, since (29) is linear, the linear error estimator presented in Section 3 can be fully extended to this nonlinear case. The philosophy of the method is identical: the only difference is that instead of the linear error equation (4), the tangent version of (28) is employed.

Once interior and patch estimates are computed, they must be measured and added. Thus, in order to completely generalize the linear case, a nonlinear energy norm must be defined. If the tangent form  $a_T(u_h; \cdot, \cdot)$  is symmetric positive definite, the reference error  $e_{\tilde{h}}$  computed using (29) is the projection of the actual error  $e$  onto  $V_{\tilde{h}}$  following the scalar product  $a_T(u_h; \cdot, \cdot)$ . Thus the norm induced by  $a_T(u_h; \cdot, \cdot)$  is taken to measure the error.

**Remark 6.** The norm induced by  $a_T(u_h; \cdot, \cdot)$  is analogous to the linear energy norm defined in (3) and is also interpreted, from a physical viewpoint, as an energetic quantity. The measure of the error can be understood as the energy needed to move the system from the state described by the approximate solution  $u_h$  to the state associated with the actual solution  $u$ .

As has already been remarked, tangent matrices can be computed in a straightforward manner and, consequently, the tangent versions of the local problems of (9) and (15) can be naturally implemented in the finite-element code. It is worth noticing that, in the patch estimation phase, the orthogonality condition of (19) must be replaced by its tangent version:

$$a_T(u_h; \eta_l, \varepsilon) = 0. \quad (30)$$

This linear restriction can also be easily implemented using the Lagrange multiplier technique.

Note that the structure and the rationale of the linear estimator is fully respected and, consequently, the nonlinear generalization inherits all the properties of its linear counterpart.

## 5. Adaptive Strategy Based on Error Estimation

The use of finite elements in practical engineering problems requires adaptive computations. The adaptive strategy employed in this work is based on two main ingredients: error estimation and  $h$ -remeshing. The error distribution of the solution computed with a given mesh is computed with the error estimator just discussed, and translated into a field of desired element sizes with the so-called optimality criterion (Díez and Huerta, 1999). An unstructured quadrilateral mesh generator (Sarrate and Huerta, 2000) is then used to build a mesh with the desired sizes. This iterative process stops (typically after 2 to 4 iterations) when the relative error of the solution (i.e. the energy norm of the error divided by the energy norm of the solution) is below a prescribed threshold set *a priori*. This adaptive procedure is illustrated in Fig. 4.

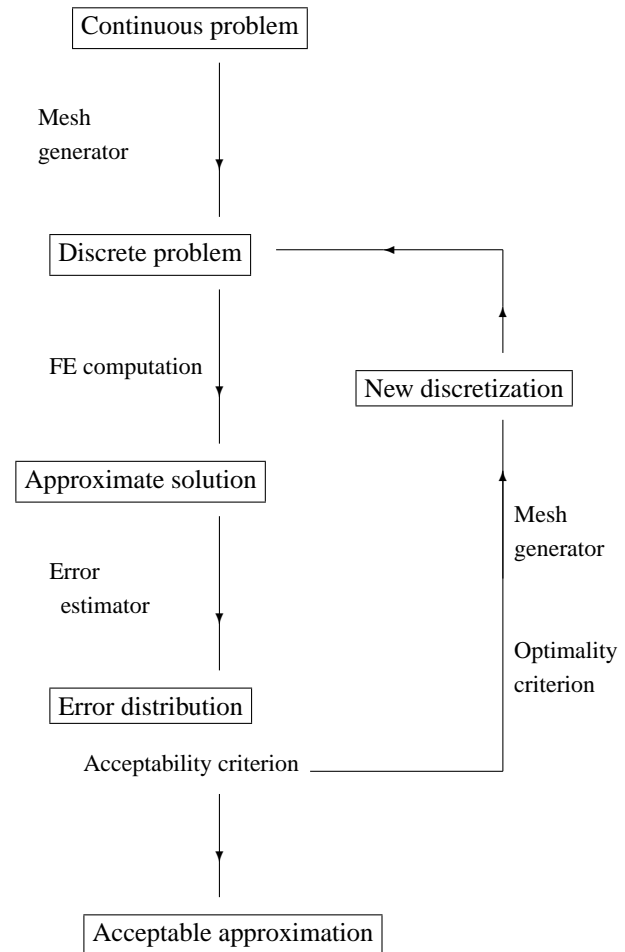


Fig. 4. The flow diagram of an adaptive procedure.

## 6. Numerical Examples

### 6.1. The Single-Edge Notched Beam

The proposed adaptive strategy is illustrated here by means of the single-edged notched beam (SENB) test (Carpinteri *et al.*, 1993). The geometry, loads and supports are shown in Fig. 5. A plane stress analysis is performed. The concrete beam is modelled with a nonlocal damage model. These models are nowadays a standard approach to modelling the failure of concrete and other quasi-brittle materials (Bažant and Pijaudier-Cabot, 1988; Mazars and Pijaudier-Cabot, 1989; Lemaitre and Chaboche, 1990; Pijaudier-Cabot and Bažant, 1987). A presentation of these models is beyond the scope of this paper and can be found elsewhere (Rodríguez-Ferran and Huerta, 2000; Rodríguez-Ferran *et al.*, 2001). Two sets of material parameters are used (Rodríguez-Ferran *et al.*, 2001). For Material 1, there is a significant post-peak softening in the stress-strain law for concrete. For Material 2, on the contrary, the softening is very slight, so the residual strength almost coincides with the peak strength (Peerlings *et al.*, 1998). The steel loading platens are assumed to be elastic.

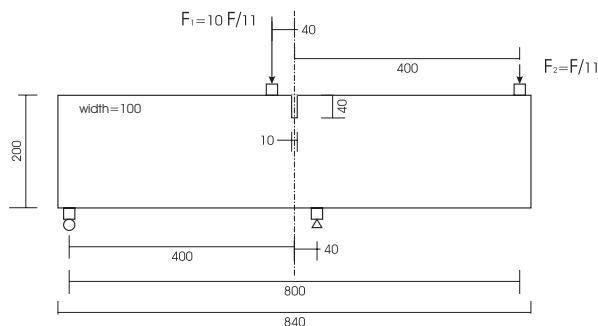


Fig. 5. Single-edge notched beam: the problem statement. All distances in mm.

#### 6.1.1. Test with Material 1

The results obtained with Material 1 are shown in Figs. 6–8. The initial mesh is shown in Fig. 6(a). Note that this mesh is relatively coarse, with only one element in the notch width. The final damage distribution and deformed mesh (amplified 300 times), corresponding to a CMSD (crack-mouth sliding displacement) of 0.08 mm, is depicted in Fig. 6(b). The curved crack pattern observed in experiments (Carpinteri *et al.*, 1993) is clearly captured. The error estimation procedure discussed in Section 4 is employed to compute the error field of Fig. 6(d). The error is larger in the damaged zone and near the loading platens. The global relative error (i.e. the energy norm of the error in displacements over the energy norm of displacements)

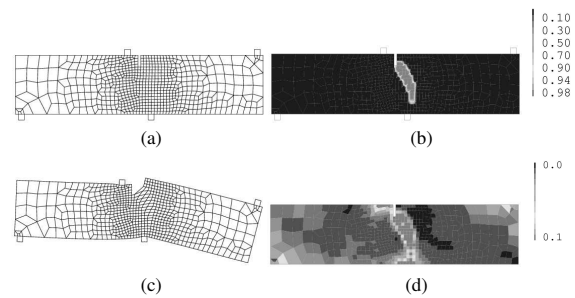


Fig. 6. SENB test with Material 1, initial approximation in the adaptive process: (a) Mesh 0: 659 elements and 719 nodes, (b) final damage distribution, (c) final deformed mesh ( $\times 300$ ), (d) error distribution. The global relative error is 3.96%.

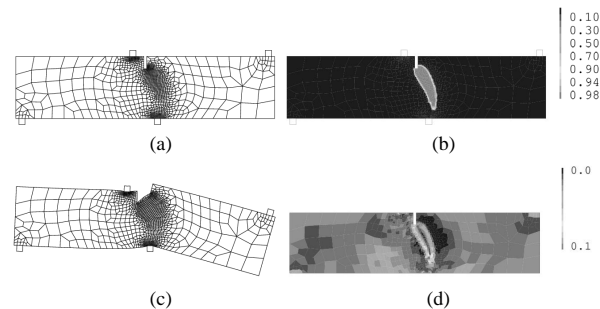


Fig. 7. SENB test with Material 1, after one iteration in the adaptive process: (a) Mesh 1: 1155 elements and 1228 nodes, (b) final damage distribution, (c) final deformed mesh ( $\times 300$ ), (d) error distribution. The global relative error is 2.11%.

is 3.96%, above a threshold of 2% set *a priori*, so adaptivity is required.

The error field of Fig. 6(d) is translated into the mesh of Fig. 7(a). Note the element concentration in the crack and the central supports. This finer mesh leads to a better definition of the damaged zone, see Fig. 7(b). The error estimator now detects that the largest errors are associated with the *edges* of the cracked zone, see Fig. 7(d). The global relative error of 2.11% is still slightly above the error goal, so another adaptive iteration is performed. The outcome of this second iteration is shown in Fig. 8. The qualitative results of Iteration 1 are confirmed: (a) small elements are needed to control the error in the damaged zones and close to the loading platens and (b) the error is larger in the edges than in the centre of the crack. The global relative error of 1.77% is below the threshold of 2%, so the adaptive iterative process stops.

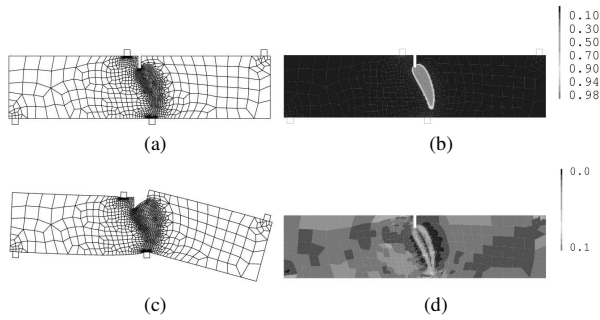


Fig. 8. SENB test with Material 1, after two iterations in the adaptive process: (a) Mesh 2: 1389 elements and 1469 nodes, (b) final damage distribution, (c) final deformed mesh ( $\times 300$ ), (d) error distribution. The global relative error is 1.77%.

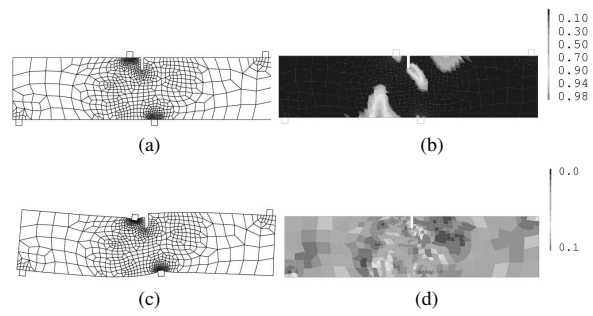


Fig. 10. SENB test with Material 2, after one iteration in the adaptive process: (a) Mesh 1: 776 elements and 848 nodes, (b) final damage distribution, (c) final deformed mesh ( $\times 300$ ), (d) error distribution. The global relative error is 2.46%.

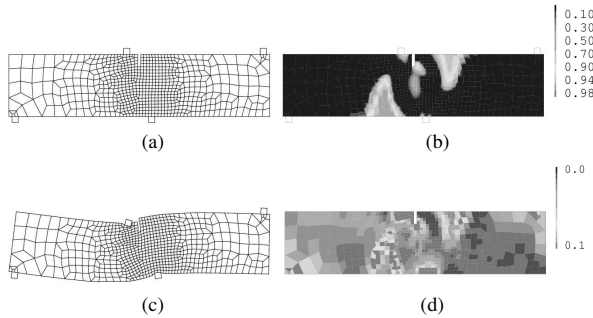


Fig. 9. SENB test with Material 2, initial approximation in the adaptive process: (a) Mesh 0: 659 elements and 719 nodes, (b) final damage distribution, (c) final deformed mesh ( $\times 300$ ), (d) error distribution. The global relative error is 3.66%.

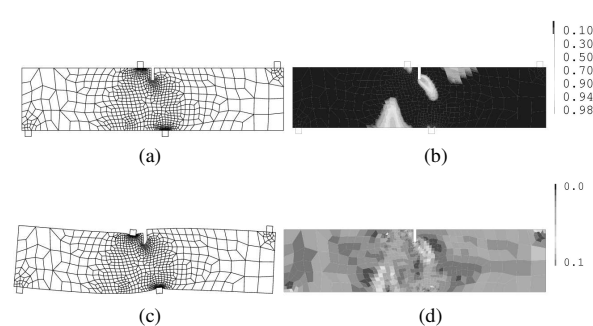


Fig. 11. SENB test with Material 2, after two iterations in the adaptive process: (a) Mesh 2: 870 elements and 954 nodes, (b) final damage distribution, (c) final deformed mesh ( $\times 300$ ), (d) error distribution. The global relative error is 2.13%.

### 6.1.2. Test with Material 2

The SENB test is now reproduced with Material 2, which has a stress-strain law with almost no softening (Rodríguez-Ferran *et al.*, 2001). A very similar law has been employed to simulate the SENB test with gradient-enhanced damage models (Peerlings *et al.*, 1998).

The results are shown in Figs. 9–11. The initial mesh is the same as before, see Fig. 9(a). The change in the material parameters leads to a completely different failure pattern, dominated by bending of opposite sign in the two halves of the beam, see Figs. 9(b) and 9(c). A crack at the notch tip is also initiated, but it is only a secondary mechanism. The error estimation procedure has no difficulties reflecting the change in the failure mode, see Fig. 9(d). The global relative error is 3.66%, so adaptivity is required.

Figures 10 and 11 illustrate the adaptive process. Note that Meshes 1 and 2 are quite different from the ones obtained with Material 1. The global relative errors are 2.46% and 2.13%. This value is still slightly above the threshold of 2%. However, an additional iteration is considered not necessary for the illustrative purposes of this test.

A final comparison between the two sets of material parameters is offered in Fig. 12, where the total load is plotted versus the CMSD for Meshes 0 and 2. The results obtained with Material 1—a peak load of around 60 kN and post-peak structural softening, see Fig. 12(a)—are in good agreement with the experiments (Carpinteri *et al.*, 1993). With Material 2, on the other hand, the peak load is quite higher and no softening is observed, see Fig. 12(b).

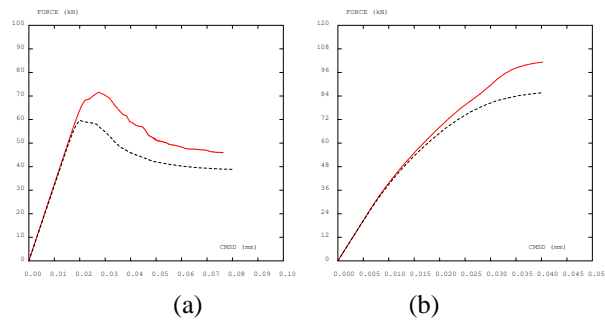


Fig. 12. Total load versus crack-mouth sliding displacement (CMSD) for Meshes 0 (solid line) and 2 (dashed line): (a) with Material 1 (large softening), (b) with Material 2 (very slight softening).

## 6.2. Adaptivity for Shells

The adaptive computation of shell structures also illustrates the application of the presented techniques to complex engineering problems. In the two presented examples the shells are assumed to exhibit nonlinear material behaviour (elasto-plastic). The error estimation strategy presented here is used to drive the adaptive procedure.

The shell element technology used in the examples is based on the Reissner-Midlin theory. However, in the thin shell regime the Reissner-Midlin model suffers from shear and membrane locking. Here, degenerated solid shell elements (Lee *et al.*, 1999) are used to obtain locking-free elements. The adopted approach is the formulation introduced by Donea and Lamain (1987). The key aspects of the generalization of the error estimator to such a kind of shell elements can be found in (Díez and Huerta, 2000).

### 6.2.1. Plastic Clamped Cylinder

Let us consider a clamped cylinder with a transversal load. The material is assumed to be elasto-plastic. Due to the symmetry of the geometry and the skew-symmetry of the load only one fourth of the specimen are analyzed. The problem statement and the deformed shape of the structure are shown in Fig. 13.

The solution exhibits strain concentration in the corners of the specimen (corresponding to the intersection of the loaded edge and the symmetry planes). The error estimator detects larger errors along the loaded edge and in an interior region. The adapted meshes are refined in these zones, where the gradient of strains is larger, see Fig. 14. After two remeshing steps, the prescribed accuracy of 3% is attained.

Radius = 1 m  
Height = 1.53m  
Thickness = 0.05 m

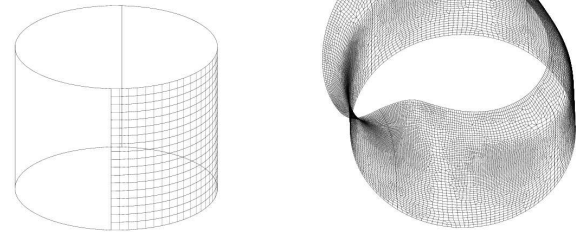


Fig. 13. Description of the clamped cylinder, geometry and deformed shape.

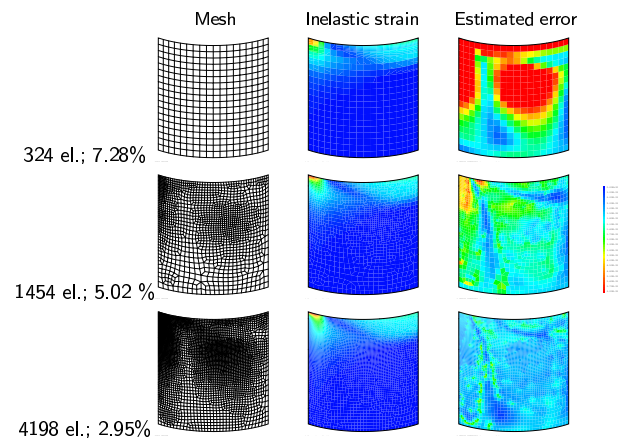


Fig. 14. Evolution of the adaptivity procedure for the clamped cylinder.

## 6.3. Cylindrical Panel with Central Opening

A cylindrical panel with a central hole is uniformly stretched. The central weakness introduced by the hole induces strain localization, see Fig. 15.

The adaptivity process driven by the error estimation strategy introduced in this paper converges to a solution with an error lower than the error threshold, which is again set to 3%. The resulting mesh concentrates small elements along the edges of the strain localization region, see Fig. 16. Again, the adaptive process refines the mesh where the strain gradients are larger, i.e. where the solution is more difficult to interpolate.

## 7. Concluding Remarks

The residual-type error estimator for nonlinear FE analysis just discussed is a straightforward generalization of the linear residual-type estimator. The nonlinear version

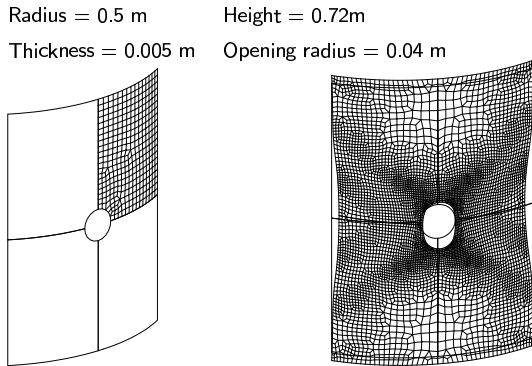


Fig. 15. Description of the cylindrical panel, geometry and deformed shape.

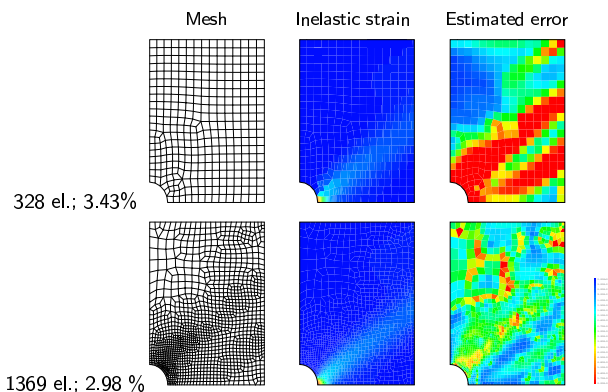


Fig. 16. Evolution of the adaptivity procedure for the cylindrical panel.

inherits all the mathematical properties of its linear counterpart. Thus the obtained estimate is a lower bound of the actual error, i.e. a systematic underestimation of the error is introduced. However, this underestimation has been found to be small. On the other hand, this estimator can be applied to a wide range of problems discretized by general unstructured meshes, even with different element types. Moreover, the efficiency of the estimator does not depend on superconvergence properties and may include the assessment of the pollution errors with a small supplementary computational effort. As regards algorithmic issues, the implementation of the estimator in a finite-element code is simple because the basic operations are performed by standard routines.

The numerical examples illustrate the efficiency of the adaptive strategy. With two sets of material parameters leading to very different failure modes,  $h$ -remeshing concentrates elements where needed according to the error estimator, until the global relative error falls below an error threshold. By keeping the discretization error under control, it is possible to ensure the quality of the FE solution and assess the influence of the material parameters in an objective way.

## References

- Ainsworth M. and Oden J.T. (1993): *A unified approach to a posteriori error estimation using element residual methods*. — Num. Math., Vol. 65, No. 1, pp. 23–50.
- Bank R.E. and Weiser A. (1985): *Some a posteriori error estimators for elliptic partial differential equations*. — Math. Comp., Vol. 44, No. 1, pp. 283–301.
- Bažant Z.P. and Pijaudier-Cabot G. (1988): *Nonlocal continuum damage localization instability and convergence*. — J. Appl. Mech., Vol. 55, No. 2, pp. 287–293.
- Carpinteri A., Valente S., Ferrara G. and Melchiorri G. (1993): *Is mode II fracture energy a real material property?* — Comp. Struct., Vol. 48, No. 3, pp. 397–413.
- Chow S.S. and Carey G.F. (1993): *Superconvergence phenomena in nonlinear two-point boundary-value problems*. — Num. Meth. Part. Diff. Eqns., Vol. 9, No. 5, pp. 561–577.
- Ciarlet P.G. (1983): *Introduction à l'analyse Matricielle et à l'optimisation*. — Paris: Masson.
- Díez P., Arroyo M. and Huerta A. (2000): *Adaptivity based on error estimation for viscoplastic softening materials*. — Mech. Cohes.-Fric. Mat., Vol. 5, No. 2, pp. 87–112.
- Díez P. and Egozcue J.J. (2001): *Probabilistic analysis of an a posteriori error estimator for finite elements*. — Math. Models Meth. Appl. Sci., Vol. 5, No. 5, pp. 841–854.
- Díez P. and Huerta A. (1999): *A unified approach to remeshing strategies for finite element  $h$ -adaptivity*. — Comp. Meth. Appl. Mech. Eng., Vol. 176, No. 1–4, pp. 215–229.
- Díez P. and Huerta A. (2000): *Error estimation for adaptive computations of shell structures*. — Révue Européenne des Éléments Finis, Vol. 9, No. 1–2, pp. 49–66.
- Díez P., Egozcue J.J. and Huerta A. (1998): *A posteriori error estimation for standard finite element analysis*. — Comp. Meth. Appl. Mech. Eng., Vol. 163, No. 1–4, pp. 141–157.
- Fourment L. and Chenot J.L. (1995): *Error estimators for viscoplastic materials: application to forming processes*. — Eng. Comp., Vol. 12, No. 5, pp. 469–490.
- Gallimard L., Ladevèze P. and Pelle J.P. (1996): *Error estimation and adaptivity in elastoplasticity*. — Int. J. Num. Meth. Eng., Vol. 39, No. 2, pp. 189–217.
- Huerta A. and Díez P. (2000): *Error estimation including pollution assessment for nonlinear finite element analysis*. — Comp. Meth. Appl. Mech. Eng., Vol. 181, No. 12, pp. 21–41.
- Huerta A., Rodríguez-Ferran A., Díez P. and J. Sarrate (1999): *Adaptive finite element strategies based on error assessment*. — Int. J. Num. Meth. Eng., Vol. 46, No. 10, pp. 1803–1818.
- Hughes T.J.R. (1987): *The finite element method*. — Stanford: Prentice Hall.
- Ladevèze P. and Rougeot Ph. (1997): *New advances on a posteriori error on constitutive relation in fe analysis*. — Comp. Meth. Appl. Mech. Eng., Vol. 150, No. 1–4, pp. 239–249.

- Ladevèze P., Pelle J.P. and Rougeot Ph. (1991): *Error estimation and mesh optimization for classical finite elements*. — Eng. Comp., Vol. 8, No. 1, pp. 69–80.
- Lamain L.G. and Donea J. (1987): *A modified representation of transverse shear in  $C^0$  quadrilateral plate elements*. — Comp. Meth. Appl. Mech. Eng., Vol. 63, No. 2, pp. 183–207.
- Lee C.K., Sze K.Y. and Lo S.H. (1999): *On using degenerated solid shell elements in adaptive refinement analysis*. — Int. J. Numer. Meth. Eng., Vol. 45, No. 6, pp. 627–659.
- Lemaitre J. and Chaboche J.-L. (1990): *Mechanics of Solid Materials*. — Cambridge: Cambridge University Press.
- Mazars J. and Pijaudier-Cabot G. (1989): *Continuum damage theory: application to concrete*. — J. Eng. Mech., Vol. 115, No. 2, pp. 345–365.
- Oden J.T., Demkowicz L., Rachowicz W. and Westermann T.A. (1989): *Toward a universal  $h$ - $p$  adaptive finite element strategy, Part 2. A posteriori error estimation*. — Comp. Meth. Appl. Mech. Eng., Vol. 77, No. 1–2, pp. 113–180.
- Ortiz M. and Quigley IV J.J. (1991): *Adaptive mesh refinement in strain localization problems*. — Comp. Meth. Appl. Mech. Eng., Vol. 90, No. 1–3, pp. 781–804.
- Peerlings R.H.J., de Borst R., Brekelmans W.A.M. and Geers M.G.D. (1998): *Gradient-enhanced damage modelling of concrete fracture*. — Mech. Cohes.-Frict. Mat., Vol. 3, No. 4, pp. 323–342.
- Pijaudier-Cabot G. and Bažant Z.P. (1987): *Nonlocal damage theory*. — J. Eng. Mech., Vol. 113, No. 10, pp. 1512–1533.
- Rodríguez-Ferran A. and Huerta A. (2000): *Error estimation and adaptivity for nonlocal damage models*. — Int. J. Solids Struct., Vol. 37, No. 48–50, pp. 7501–7528.
- Rodríguez-Ferran A., Arbós I. and Huerta A. (2001): *Adaptive analysis based on error estimation for nonlocal damage models*. — Revue européenne des éléments finis (Special issue: Numerical Modelling in Damage Mechanics), Vol. 10, No. 2–4, pp. 193–207.
- Sarrate J. and Huerta A. (2000): *Efficient unstructured quadrilateral mesh generation*. — Int. J. Num. Meth. Eng., Vol. 49, No. 10, pp. 1327–1350.
- Strouboulis T. and Haque K.A. (1992a): *Recent experiences with error estimation and adaptivity, Part i: Review of error estimators for scalar elliptic problems*. — Comp. Meth. Appl. Mech. Eng., Vol. 97, No. 3, pp. 399–436.
- Strouboulis T. and Haque K.A. (1992b): *Recent experiences with error estimation and adaptivity, Part ii: Error estimation for  $h$ -adaptive approximations on grids of triangles and quadrilaterals*. — Comp. Meth. Appl. Mech. Eng., Vol. 100, No. 3, pp. 359–430.
- Zhu J.Z. (1997): *A posteriori error estimation—the relationship between different procedures*. — Comp. Meth. Appl. Mech. Eng., Vol. 150, No. 1–4, pp. 411–422.
- Zienkiewicz O.C. and Huang G.C. (1990): *A note on localization phenomena and adaptive finite-element analysis in forming processes*. — Comm. Appl. Num. Meth., Vol. 26, No. 8, pp. 71–76.
- Zienkiewicz O.C. and Zhu J.Z. (1987): *A simple error estimator and adaptive procedure for practical engineering analysis*. — Int. J. Num. Meth. Eng., Vol. 24, No. 1, pp. 337–357.